Dispersion Interactions and Vibrational Effects in Ice as a Function of Pressure: A First Principles Study

Éamonn D. Murray and Giulia Galli

Department of Chemistry, University of California, Davis, California 95616, USA

(Received 12 November 2011; revised manuscript received 19 January 2012; published 5 March 2012)

We present a first principles theoretical framework that accurately accounts for several properties of ice, over a wide pressure range. In particular, we show that, by using a recently developed nonlocal van der Waals functional and by taking into account hydrogen zero point motion, one can properly describe the zero temperature equation of state, the vibrational spectra, and the dielectric properties of ice at low pressure and of ice VIII, a stable phase between 2 and 60 GPa. While semilocal density functionals yield a transition pressure from ice XI to VIII that is overestimated by almost an order of magnitude, we find good agreement with experiments when dispersion forces are taken into account. Zero point energy contributions do not alter the computed transition pressure, but they affect structural properties, including equilibrium volumes and bulk moduli.

DOI: 10.1103/PhysRevLett.108.105502 PACS numbers: 63.20.dk, 62.50.−p, 71.15.Mb, 83.80.Nb

Ice has an extremely complex phase diagram [1] that has been studied for over a century [2], due to its importance in several disciplines, encompassing physics, chemistry, and earth and atmospheric sciences. However, until about 35 years ago, little was known experimentally about high pressure phases of ice. For example, the first characterization of ice VIII as an antiferroelectric, ordered phase—now known to be stable at low temperature between 2 and 60 GPa—appeared in 1976 [3]. From a theoretical standpoint, the description of the phase diagram and the properties of ice remains a very challenging problem. Recent *ab initio* calculations [4,5] have reported remarkable progress in describing the equations of state of some ice phases within density functional theory, as well as in computing optical spectra [6,7]. However, no first principles theory has yet successfully predicted with consistent accuracy a wide range of properties encompassing structural, vibrational, and dielectric properties over a broad range of pressures.

In this Letter, we focus on ordered ice phases, ice XI, ordered cubic ice I_c, and ice VIII. Ice XI and ordered I_c are used as models of the stable phase of ice at ambient pressure close to 0 °C. We show that a proper account both of dispersion forces and of hydrogen zero point motion are necessary to obtain a consistently accurate description of several properties of ice over a wide pressure range, at low temperature. We thus establish a theoretical framework that can be used to gain insight into the intricate physics of ice as a function of pressure, from first principles.

We carried out calculations within density functional theory and compared results obtained with semilocal (PBE [8]) and nonlocal van der Waals (vdW-DF2 [9]) functionals. We used the QUANTUM ESPRESSO package [10] with hard norm-conserving pseudopotentials [11] for both hydrogen and oxygen and a plane-wave energy cutoff of 160 Ry. A $4 \times 4 \times 4$ k-point grid was used for each structure.

The lattice energies and equilibrium volumes of each phase were calculated by fully relaxing internal coordinates and cell parameters [12]. The bulk modulus B_0 and its pressure derivative B_0' were obtained by relaxing each structure to a series of five target pressures, from −1.0 to 1.0 GPa, and fitting our data to the third-order Birch-Murnaghan equation of state [13].

Our results are presented in Table I. The close agreement between our calculations for ordered I_c and ice XI show the insensitivity of the $T = 0$ equation of state to proton ordering. We have also performed the same calculations using the 12-molecule hexagonal ice model of Ref. [20] as used in the other theoretical studies cited and found equation-of-state parameters in similarly close agreement [21]. At both the PBE and vdW-DF2 level of theory, the computed structural properties are in satisfactory agreement with experiments. PBE calculations underestimate the equilibrium volume of ice I_h by 4.8%, while vdW-DF2 overestimates it by 3.8%. These differences with respect to the measured value are expected to be rather insensitive to temperature, due to the small thermal expansion coefficient of ice at low P; for example, the measured volume change in I_h from 10 to 265 K is 1.65% [18,22]. In the case of ice VIII, PBE and vdW-DF2 results overestimate the measured equilibrium volume by 1.8% and 4.5%, respectively. Note the consistent overestimate of volumes by vdW-DF2 for both low and high pressure phases and errors on volumes of different sign when using PBE. In general, our PBE results are in good agreement with previous calculations [14,17]. However, we find a noticeably lower (∼ 20%) bulk modulus in ice VIII when compared to the results of Ref. [17], mostly due to a larger equilibrium volume obtained in this work (we expect the difference to originate from the use of a harder pseudopotential). Our I_h results show a moderate improvement

TABLE I. Calculated values of the structural properties of ice XI, I_c, and VIII, by using semilocal (PBE) and van der Waals functionals (vdW-DF2), compared to measured values (bold) and previous calculations (italic) using van der Waals (RPBE + vdW-DF) and hybrid (PBE0) functionals and quantum Monte Carlo calculations (DMC).

	E_1 (eV)	V_0 (cm^3/mol)	B_0	B_0'
I_h				
XI PBE	−0.663	18.37	14.60	5.7
XI vdW-DF2	−0.649	20.01	12.59	5.2
I_c PBE	−0.663	18.37	14.67	5.7
I_c vdW-DF2	−0.648	20.05	12.96	5.6
Experiment[a]	**−0.610**	**19.30**	**12.1**	**5.5**
PBE [14]	*−0.64*	*18.46*		
RPBE + vdW-DF [4]	*−0.60*	*20.48*		
DMC [5]	*−0.605*	*19.08*	*18.3*	
PBE0 + vdW^{TS} [5]	*−0.672*			
Ice VIII				
PBE	−0.485	12.31	16.55	6.1
vdW-DF2	−0.620	12.65	20.76	5.7
Experiment [15,16]	**−0.577**	**12.1**	**27.9**	**3.6**
PBE [17]		*12.12*	*20.09*	*5.01*
DMC [5]	*−0.575*	*11.72*	*23.8*	

[a]Reference [16], Ref. [18], Ref. [19] extrapolated value at 0 K, and Ref. [15].

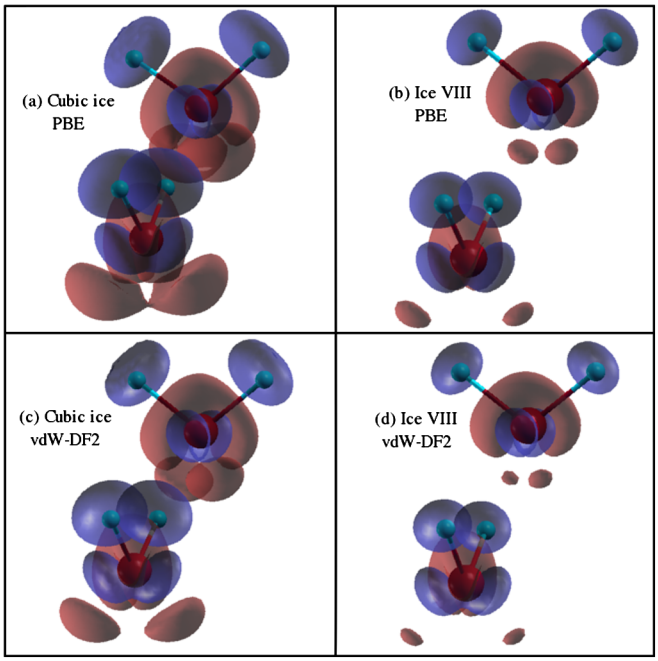

FIG. 1 (color online). The change in electronic density in cubic ice and ice VIII with respect to a free water molecule as calculated with semilocal (PBE) and van der Waals (vdW-DF2) functionals. Pink and blue isosurfaces (all chosen at the same value) show regions where the density is increased and decreased, respectively. Oxygen and hydrogen atoms are indicated as red and cyan balls, respectively.

over those of Ref. [4], where an approach based on vdW-DF [23] with a different exchange functional was used. Recent diffusion Monte Carlo (DMC) results [5] yield lattice energies in closest agreement with experiment. They appear to slightly underestimate the equilibrium volume possibly due to the absence of vibrational effects (as discussed below); this yields larger bulk moduli than obtained with other methods, with a value in excellent agreement with experiment for ice VIII [15] but an overestimate of experiment for ice I_h.

We find substantial differences in the intramolecular bonding in the low and high pressure ice phases, as seen in Fig. 1 showing the difference of the charge densities ($\Delta\rho$) of ice I_c and VIII with respect to those of free water molecules. At high pressure, ($\Delta\rho$)'s are predominantly localized in proximity of the molecules, indicating a substantial weakening of hydrogen bonds upon compression, which is likely accompanied by a change in the relative contributions of hydrogen bonding and dispersion forces to intermolecular interactions. This weakening has been indicated by previous Raman measurements on ice [24] and recent calculations of the O-H stretch frequency [5]. Consistent with hydrogen bond weakening, we find a change of the molecular dipole moment (μ) at high pressure [25]. When using PBE (vdW-DF2), μ is reduced from 3.51 (3.23) D in ice XI to 2.95 (2.86) in ice VIII. The dipole strengths obtained for ordered I_c are very close to those of ice XI.

We next investigated the effect of zero point motion on our results, by adding to the total energy the contribution from the vibrational energy: $E_{\text{vib}} = \frac{1}{2N_q}\sum_{q,\nu}\hbar\omega_{q,\nu}(n + 1/2)$; N_q is the total number of phonon wave vectors, and $\omega_{q,\nu}$ is the frequency of mode ν at wave vector q. We computed the dynamical matrix for each phase on a $4 \times 4 \times 4$ grid by using density functional perturbation theory. We then obtained frequencies over a $12 \times 12 \times 12$ grid via Fourier interpolation, with the acoustic sum rule enforced to ensure that the translational modes go to zero at the Γ point. The phonon density of states for ice XI and ice VIII are shown in Fig. 2. PBE and vdW-DF2 results exhibit several differences in the low P phase. The stretching mode frequencies are higher in ice XI and I_c when using vdW-DF2, consistent with results obtained for liquid water [26] and in better agreement with the peaks observed in the measured IR spectra [27], at 3150, 3220, and 3380 cm^{-1}. Differences between the phonon density of states of ice VIII obtained at the PBE and vdW-DF2 level of theory are instead minor. Recent Raman measurements of the stretching vibrations [15] indicate that the frequencies are approximately 3350, 3440, and 3470 cm^{-1}, consistent with our calculations. The bending modes show little change with respect to either phase or functional, and the rotational and translation modes are redshifted when using vdW-DF2, with respect to PBE results.

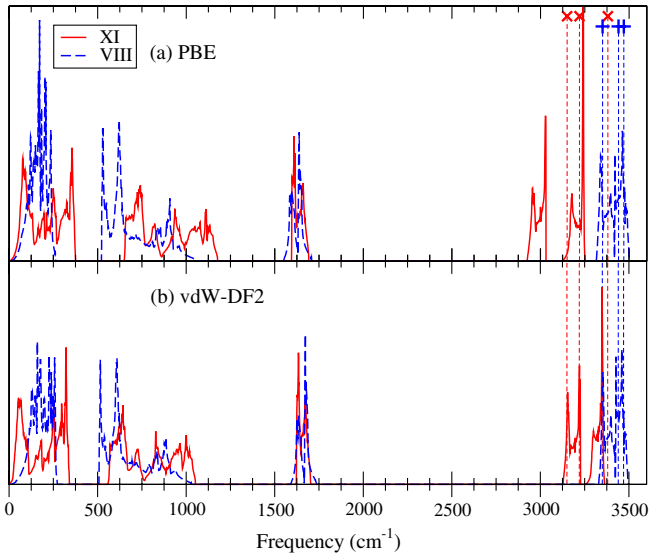

FIG. 2 (color online). The phonon density of states for ice XI (red solid line) and VIII (blue dashed line) calculated by using (a) PBE and (b) vdW-DF2 functionals (see the text). Calculations for I_c agree closely with those of ice XI and are omitted. × and + symbols indicate experimentally measured peaks for hexagonal ice and ice VIII, respectively.

Assuming that the Gruneisen parameter $\gamma_{q,\nu}$ of each phonon mode is constant for small variations (1%–2%) in volume (V), E_{vib} varies linearly with V. Therefore, the free energy $F = E + E_{\mathrm{vib}}$ has a minimum at a value of V slightly shifted from the optimized volume (V_0) reported in Table I; in addition, a small increase in the binding energy is expected, compared to the value computed by simply adding $E_{\mathrm{vib}}(V_0)$ to the energy calculated at V_0. At 0 K, we fitted $E_{\mathrm{vib}}(V)$ with a linear function and numerically solve $\frac{dF}{dV} = 0$. This is equivalent to calculating the Gruneisen parameter of each mode and finding the contribution from each mode and wave vector individually.

The volume dependence of E_{vib} and of the Gruneisen parameters are calculated by homogeneously expanding or contracting lattice vectors; the ionic positions are then relaxed and the dynamical matrix evaluated. Derivatives with respect to V are computed by a linear fit over five volume values. Bulk moduli and their pressure derivatives corrected for vibrational effects are obtained from the second and third derivatives of the Birch-Murnaghan equation of state. $E_{\mathrm{vib}}(V)$ is linear over the small range of volumes under consideration, and thus it does not contribute to the second or third derivative of $F(V)$.

The results of our calculations inclusive of zero point energy (ZPE) contributions are reported in Table II, where they are compared to previous experimental and theoretical results. The inclusion of ZPE affects only the binding energy of the low pressure phases at the PBE level, while it also affects the equilibrium volume (increased by ~2%) at the vdW level of theory and the bulk modulus. With both functionals, the inclusion of ZPE substantially impacts the calculated properties of ice VIII, leading to a 6% increase in the volume and a 25% decrease in the bulk modulus, in good agreement with the trend observed in Ref. [17] by using PBE. The inclusion of the ZPE worsens the agreement with experiment [15], primarily because of the volume overestimate [28]. We note the much better agreement with experiment obtained for the binding energy of ice VIII when using the vdW functional. This result, together with the energy difference between ice XI and ice VIII computed with PBE and vdW-DF2 (0.178 and 0.029 eV, respectively), shows that PBE overestimates the stability of phases that are mostly hydrogen bonded, with respect to those where hydrogen bonding is weaker and dispersion forces play a more important role. These findings are consistent with those of a recent study of water [26].

TABLE II. Calculated values of the structural properties of ice XI, I_c, and VIII, obtained by adding zero point motion contributions to the values reported in Table I. Measured values (bold) and previous PBE calculations (italic) are given for comparison, when available. ΔV indicates the volume change relative to the value listed in Table I.

	E_l (eV)	V_0 (cm^3/mol)	ΔV (%)	B_0 (GPa)	B_0'
I_h					
XI PBE	−0.535	18.41	0.2	14.43	5.7
XI vdW-DF2	−0.520	20.33	1.5	11.59	5.3
I_c PBE	−0.535	18.44	0.4	14.32	5.7
I_c vdW-DF2	−0.518	20.44	1.9	11.61	5.8
Experiment[a]	**−0.491**	**19.30**		**12.1**	**5.5**
Ice VIII					
PBE	−0.364	13.16	6.9	10.76	6.9
vdW-DF2	−0.492	13.38	5.8	14.83	6.3
Experiment[b]		**12.1**		**27.9**	**3.6**
PBE[c]		*12.85*	*6.0*	*15.91*	*4.95*

[a]Reference [16], Ref. [18], Ref. [19] extrapolated value at 0 K, and Ref. [15].
[b]Reference [16] and Ref. [15].
[c]Reference [17].

By evaluating $E_{\mathrm{vib}}(V)$ at $T = 0$ for both H_2O and D_2O ice systems, we can obtain the volume isotope effect (VIE). This effect arises when changing the mass of the hydrogen atom, which leads to a change in vibrational frequencies and in turn to a volume variation. Our results are shown in Table III.

The measured VIE for I_h is +0.09% [18]. While our vdW-DF2 result is negative, the error with respect to the measured value is significantly smaller than that of PBE. The computed VIE at low P is likely subject to substantial numerical errors, as the calculated vibrational corrections to the volume are rather small for ice XI and I_c [29]. Interestingly, we do find a reverse isotope shift of over 1% in ice VIII that appears to be robust against the inclusion of dispersion interactions. Because of a significantly larger volume correction due to vibrational effects in ice VIII, we expect the calculated isotope shift to be

TABLE III. Calculated molar volume, VIE, and bulk modulus at $T = 0$ for the deuterated versions of ice XI, I_c, and ice VIII.

	V_0 (cm^3/mol)	VIE (%)	B_0 (GPa)
XI PBE	18.48	0.4	14.09
XI vdW-DF2	20.32	−0.03	11.60
I_c PBE	18.51	0.4	14.01
I_c vdW-DF2	20.43	−0.06	11.66
VIII PBE	13.00	−1.2	11.71
VIII vdW-DF2	13.22	−1.2	15.93

numerically more robust at high P. A negative VIE is to be expected in a non-hydrogen-bonded system—for example, a value of −1% is measured for LiH [31]; therefore, the calculated negative VIE for ice VIII is a further indication of the weakening of hydrogen bonding at high pressure.

We calculated the transition pressure between ice XI and ice VIII as $-\Delta E/\Delta V$. The values obtained without (with) ZPE contributions are 2.84 (3.14) GPa and 0.38 (0.38) GPa with PBE and vdW-DF2, respectively, to be compared with the measured value of 0.40 GPa [16]. The transition pressure obtained with vdW-DF2 is remarkably close to the experimental result and about an order of magnitude better than the PBE prediction. A good agreement with experiment was also seen in recent diffusion Monte Carlo calculations [5] (0.39 GPa), while the inclusion of vdW dispersion forces based on an atomiclike description [32] yielded an overestimate of the transition pressure by a factor of ∼3. Our findings show that the vdW-DF2 level of theory provides a far more consistent description of the equation of state of both the low and the high pressure phases of ice than PBE and other known *ab initio* descriptions of dispersion forces within a density functional theory approach.

We now turn to the discussion of the electronic and dielectric properties of ice; these have so far received little attention within the theoretical community performing first principles computations. In particular, no *ab initio* calculations of dielectric constants of ice have been reported in the literature, in spite of their importance, e.g., in geophysical modeling [33]. As expected at both the PBE and vdW-DF2 level, we obtain electronic gaps that are underestimated with respect to experiment: 5.58 and 5.18 eV in the ice XI and VIII phases, respectively, with PBE and 5.04 and 5.12 eV with vdW-DF2. The measured gap of ice I_h is 10.9 eV [34]. Interestingly, the gap decreases upon compression with PBE, while it increases with vdW-DF2. From the recent work of Ref. [7] on optical properties of ice based on many-body perturbation theory, one would expect the band gap to increase with pressure.

At low P, the high frequency macroscopic dielectric constant is in good agreement with experiment with both PBE and vdW-DF2 functionals (see Table IV [39]) and about 20% smaller than at high P. The low frequency dielectric constants (ϵ_M^0) exhibit instead a non-negligible dependence on the functional, in part because of the difference in vibrational spectra (see Fig. 2). The ϵ_M^0 of ice VIII appears to be in better agreement with experiment when evaluated by using vdW-DF2. We note the substantial anisotropy found in the low frequency ϵ due to the orientation of the molecular dipoles in the cell. This is particularly prominent in ice VIII due to its antiferroelectric structure.

TABLE IV. Calculated values of the macroscopic high frequency dielectric constant $\epsilon_M^\infty = 1/\epsilon_{0,0}^{-1}(0)$ and the low frequency dielectric constant ϵ_M^0 compared to measurements obtained via the optical response and the response at ∼1 MHz (bold).

	ϵ_M^∞	ϵ_M^0		
		xx	*yy*	*zz*
I_h Expt[a]	**1.72**		**3.09**	
XI PBE	1.83	3.31	2.73	2.58
XI vdW-DF2	1.78	2.83	2.44	2.38
ice VIII Expt[b]	**2.06**		**4.06**	
VIII PBE	2.32	4.52	4.52	2.53
VIII vdW-DF2	2.27	4.30	4.30	2.46

[a]Reference [35] and Ref [36].
[b]Reference [37] (for ice VII extrapolated to $P = 0$) and Ref. [38].

In conclusion, we have shown that, by using nonlocal van der Waals functionals, in particular, vdW-DF2, and by including zero point energy contributions, one may obtain an accurate description of several properties of ice over a wide pressure range. Therefore, such a functional appears to be a promising candidate to study ices and water under pressure and to be used in molecular dynamics simulations to explore the H_2O phase diagram as a function of T and P. All of the results obtained within PBE confirm that this semilocal functional substantially overestimates the strength of hydrogen bonding in ice. In the low pressure phase, this leads to too small a volume, too large a molecular dipole and dielectric constant, and an overestimate of the effect of hydrogen isotope mass on the structure. The use of vdW-DF2 largely rectifies these deficiencies, although it appears to slightly underestimate the strength of hydrogen bonding at low pressure. The quality of results obtained here with vdW-DF2 for the transition pressure, change in energy and volume between phases, and the bulk modulus are comparable to those reported by recent DMC calculations, which are, however, computationally much heavier than any *ab initio* calculations with nonlocal functionals.

This research was supported by SciDac-e Grant No. DE-FC02-06ER25777, by the National Science Foundation through TeraGrid resources provided by TACC and NICS under Grants No. TG-ASC090004 and No. TG-MCA06N063, and by NERSC, which is supported by the Office of Science of the U.S. Department of Energy under Contract No. DE-AC02-05CH11231. We thank P. H. Allen, C. Zhang, and F. Gygi for useful discussions.

[1] J.-Y. Chen and C.-S. Yoo, Proc. Natl. Acad. Sci. U.S.A. **108**, 7685 (2011).
[2] P. W. Bridgman, Proc. Am. Acad. Arts Sci. **47**, 441 (1912).
[3] P. T. T. Wong and E. Whalley, J. Chem. Phys. **64**, 2359 (1976).
[4] I. Hamada, J. Chem. Phys. **133**, 214503 (2010).
[5] B. Santra, J. Klimes, D. Alfè, A. Tkatchenko, B. Slater, A. Michaelides, R. Car, and M. Scheffler, Phys. Rev. Lett. **107**, 185701 (2011).
[6] V. Garbuio, M. Cascella, L. Reining, R. DelSole, and O. Pulci, Phys. Rev. Lett. **97**, 137402 (2006).
[7] A. Hermann and P. Schwerdtfeger, Phys. Rev. Lett. **106**, 187403 (2011).
[8] J. P. Perdew, K. Burke, and M. Ernzerhof, Phys. Rev. Lett. **77**, 3865 (1996).
[9] K. Lee, E. D. Murray, L. Kong, B. I. Lundqvist, and D. C. Langreth, Phys. Rev. B **82**, 081101 (2010).
[10] P. Giannozzi, S. Baroni, N. Bonini, M. Calandra, R. Car, C. Cavazzoni, D. Ceresoli, G. L. Chiarotti, M. Cococcioni, I. Dabo, A. Dal Corso, S. de Gironcoli, S. Fabris, G. Fratesi, R. Gebauer, U. Gerstmann, C. Gougoussis, A. Kokalj, M. Lazzeri, L. Martin-Samos, N. Marzari, F. Mauri, R. Mazzarello, S. Paolini, A. Pasquarello, L. Paulatto, C. Sbraccia, S. Scandolo, G. Sclauzero, A. P. Seitsonen, A. Smogunov, P. Umari, and R. M. Wentzcovitch, J. Phys. Condens. Matter **21**, 395502 (2009).
[11] Obtained from http://fpmd.ucdavis.edu, generated by using the method in D. Vanderbilt, Phys. Rev. B **32**, 8412 (1985).
[12] All calculations were performed self-consistently. Forces were converged to within 10^{-5} Ry/Bohr and the stresses to within 0.5 MPa and fully include the contributions from the vdW-DF2 functional. The lattice energies were obtained by subtracting from the total energies of the crystal the sum of energies of isolated molecules obtained in a $35 \times 35 \times 35$ Bohr cell.
[13] $P(V) = \frac{3}{2}B_0[(\frac{V_0}{V})^{7/3} - (\frac{V_0}{V})^{5/3}]\{1 + \frac{3}{4}(B_0' - 4)[(\frac{V_0}{V})^{2/3} - 1]\}$.
[14] P. J. Feibelman, Phys. Chem. Chem. Phys. **10**, 4688 (2008).
[15] Y. Yoshimura, S. T. Stewart, M. Somayazulu, H. kwang Mao, and R. J. Hemley, J. Chem. Phys. **124**, 024502 (2006).
[16] E. Whalley, J. Chem. Phys. **81**, 4087 (1984).
[17] K. Umemoto and R. M. Wentzcovitch, Phys. Rev. B **69**, 180103 (2004).
[18] K. Röttger, A. Endriss, J. Ihringer, S. Doyle, and W. F. Kuhs, Acta Crystallogr. Sect. B **50**, 644 (1994).
[19] P. H. Gammon, H. Kiefte, and M. J. Clouter, J. Phys. Chem. **87**, 4025 (1983).
[20] D. R. Hamann, Phys. Rev. B **55**, R10 157 (1997).
[21] The structure used in previous first principles work [4,5,14,20] is very close to ice XI, differing only in the in-plane proton ordering in the hexagonal structure.
[22] R. Feistel and W. Wagner, J. Phys. Chem. Ref. Data **35**, 1021 (2006).
[23] M. Dion, H. Rydberg, E. Schröder, D. C. Langreth, and B. I. Lundqvist, Phys. Rev. Lett. **92**, 246401 (2004).
[24] B. Minceva-Sukarova, W. F. Sherman, and G. R. Wilkinson, J. Phys. C **17**, 5833 (1984).
[25] We computed dipole moments using maximally localized Wannier functions calculated by using the WANNIER 90 code: A. A. Mostofi, J. R. Yates, Y.-S. Lee, I. Souza, D. Vanderbilt, and N. Marzari, Comput. Phys. Commun. **178**, 685 (2008).
[26] C. Zhang, J. Wu, G. Galli, and F. Gygi, J. Chem. Theory Comput. **7**, 3054 (2011).
[27] J. E. Bertie and E. Whalley, J. Chem. Phys. **40**, 1637 (1964).
[28] Using our computed equation of state with vdW-DF2 and the measured volume yields a value of $B = 26.5$ GPa, very close to the measured value of 27.9 GPa.
[29] The VIE of I_h obtained in recent path-integral molecular dynamics [30] simulations, -0.6%, is much larger than experiment and of the opposite sign, possibly due to the interatomic potential (TIP4P) used in the simulation.
[30] C. P. Herrero and R. Ramírez, J. Chem. Phys. **134**, 094510 (2011).
[31] P. Loubeyre, R. Le Toullec, M. Hanfland, L. Ulivi, F. Datchi, and D. Hausermann, Phys. Rev. B **57**, 10 403 (1998).
[32] A. Tkatchenko and M. Scheffler, Phys. Rev. Lett. **102**, 073005 (2009).
[33] E. Wasserman, B. Wood, and J. Brodhol, Geochim. Cosmochim. Acta **59**, 1 (1995).
[34] K. Kobayashi, J. Chem. Phys. **87**, 4317 (1983).
[35] G. P. Johari and S. J. Jones, Proc. R. Soc. A **349**, 467 (1976).
[36] S. R. Gough, Can. J. Chem. **50**, 3046 (1972).
[37] A. Dewaele, J. H. Eggert, P. Loubeyre, and R. Le Toullec, Phys. Rev. B **67**, 094112 (2003).
[38] G. P. Johari, A. Lavergne, and E. Whalley, J. Chem. Phys. **61**, 4292 (1974).
[39] Dielectric constants are obtained as described in Ref. [40]. The average diagonal component is given for ϵ_M^∞; individual components are within 1% of this value. xx, yy, and zz indicate components of the tensor along Cartesian directions for ϵ_M^0. Off-diagonal components are negligible except in the ice VIII case, where xy is -0.87 (-0.80) for PBE (vdW-DF2).
[40] X. Gonze and C. Lee, Phys. Rev. B **55**, 10 355 (1997).